Supporting Information

Sobotzik et al. 10.1073/pnas.0909267106

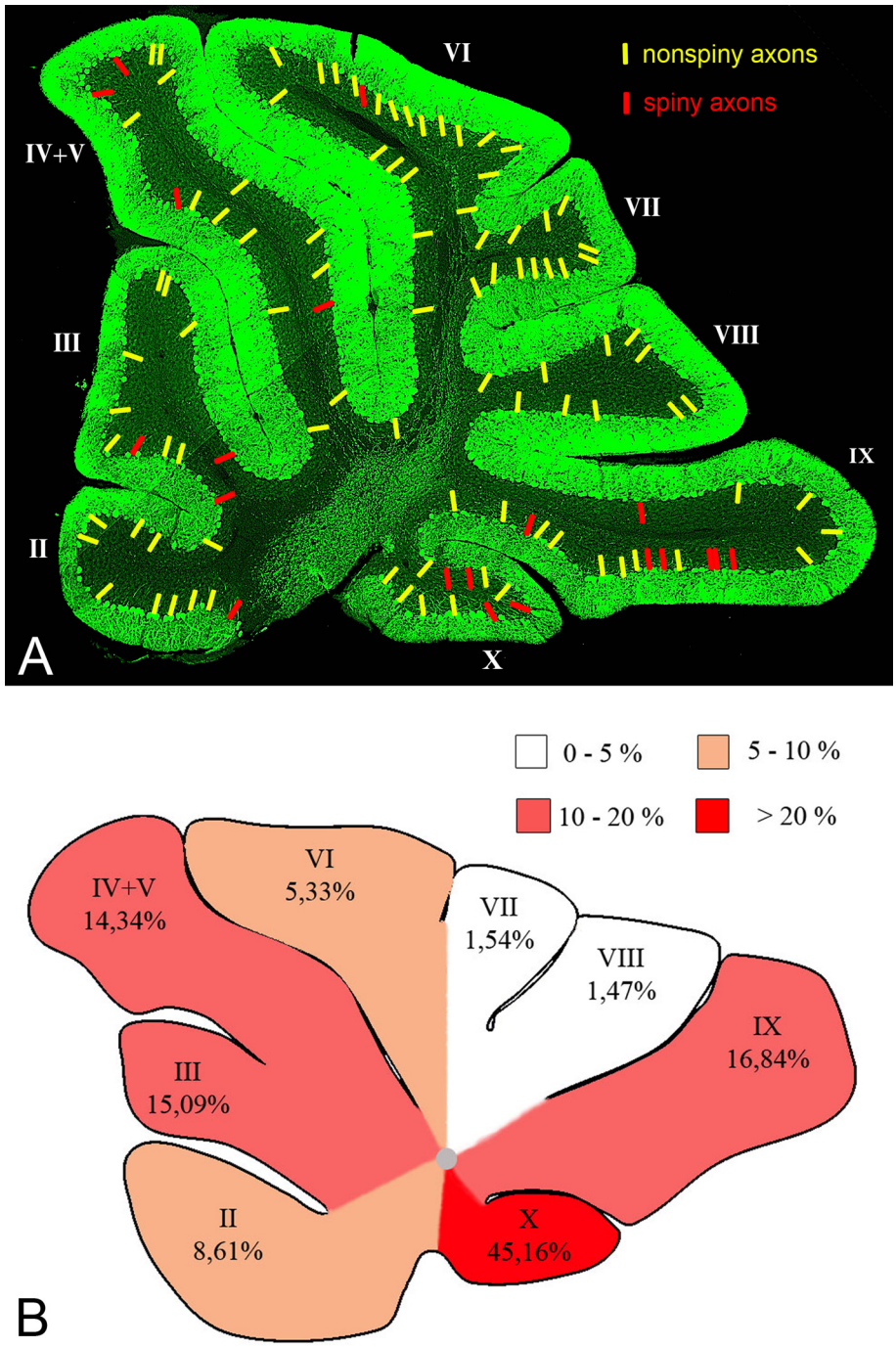

Fig. S1. Distribution and prevalence of spiny axons in ankG$^{-/-}$ mice. (*A*) Paravermal sagittal section of an ankG-deficient cerebellum. Red lines denote spiny axons, and yellow lines denote nonspiny axons. Only axons that could be traced from their parental PC soma for a distance of at least 50 μm were included. (*B*) The average percentage of spiny axons was assessed in 3 ankG$^{-/-}$ mice. A total of 1,756 axons in 3 ankG$^{-/-}$ mice and 1,378 axons in 3 age-matched ankG$^{+/+}$ mice were analyzed. Note preferential clustering of spiny axons in lobule X where 45% of all examined axons (56 of 124) possessed spines.

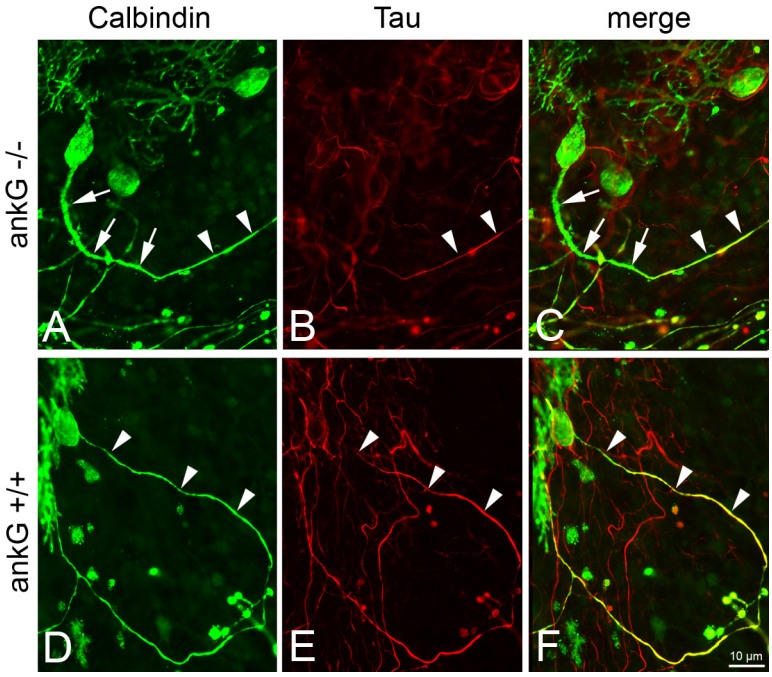

Fig. S2. Loss of tau protein in spiny segments of ankG$^{-/-}$ PC axons (cerebellar slice cultures, DIV10). (*A–C*) The spiny segment of an ankG-deficient PC axon is denoted by arrows. Arrowheads point to the subsequent nonspiny segment of the same axon. As demonstrated in the merged picture in *C*, the spiny segment of this axon is virtually devoid of tau protein whereas normal tau accumulation is seen in the nonspiny segment of this process. (*D–F*) Normal enrichment of tau protein observed in a PC axon of a control animal (arrowheads.) (Scale bar, 10 μm.)

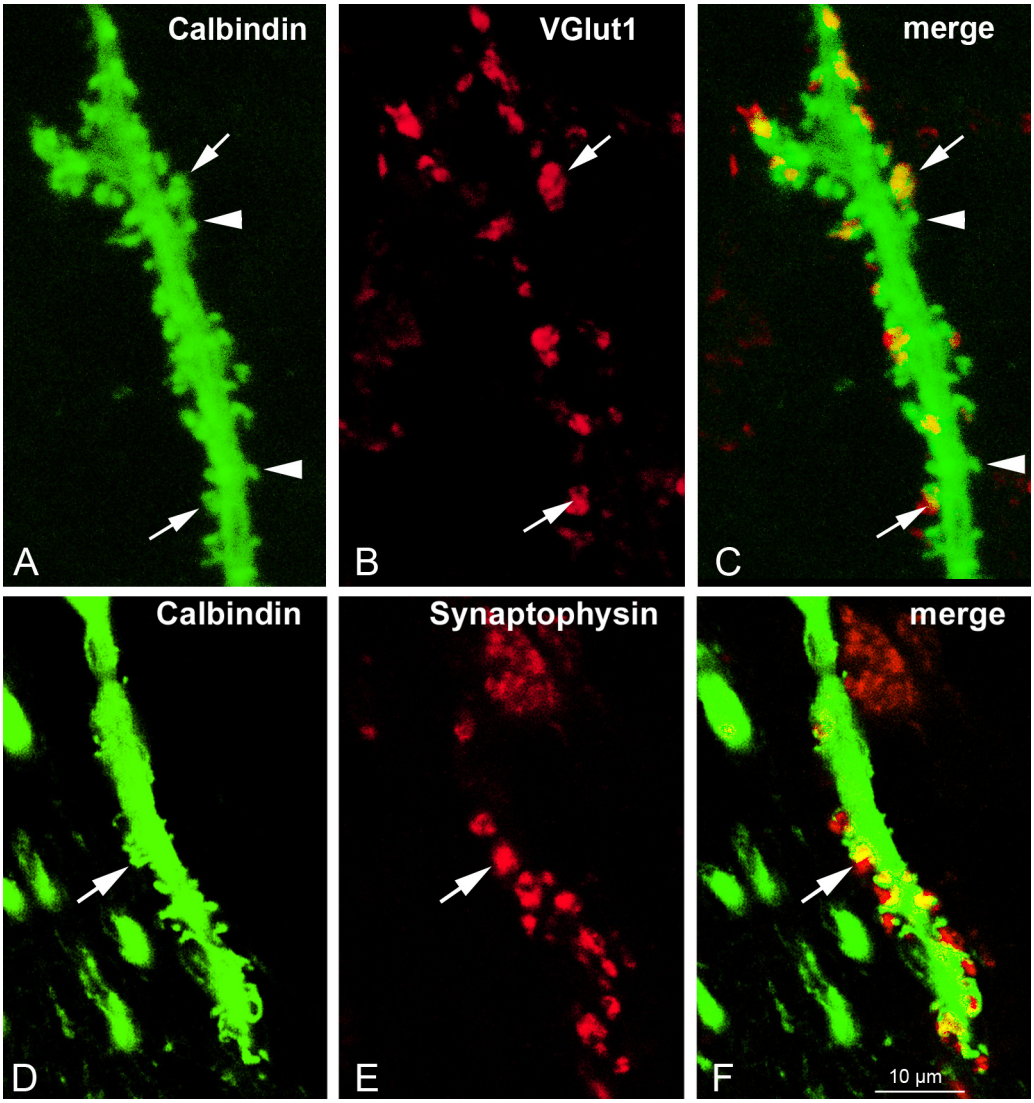

Fig. S3. Synaptic features of axonal spines in ankG$^{-/-}$ mice. (*A–C*) Axonal spines are contacted by VGlut1-positive boutons (arrows). A subset of axonal spines is devoid of glutamatergic boutons (arrowheads). (*D–F*) Axonal spines are contacted by boutons positive for synaptophysin, a marker for synaptic vesicles. (Scale bar, 10 μm.)

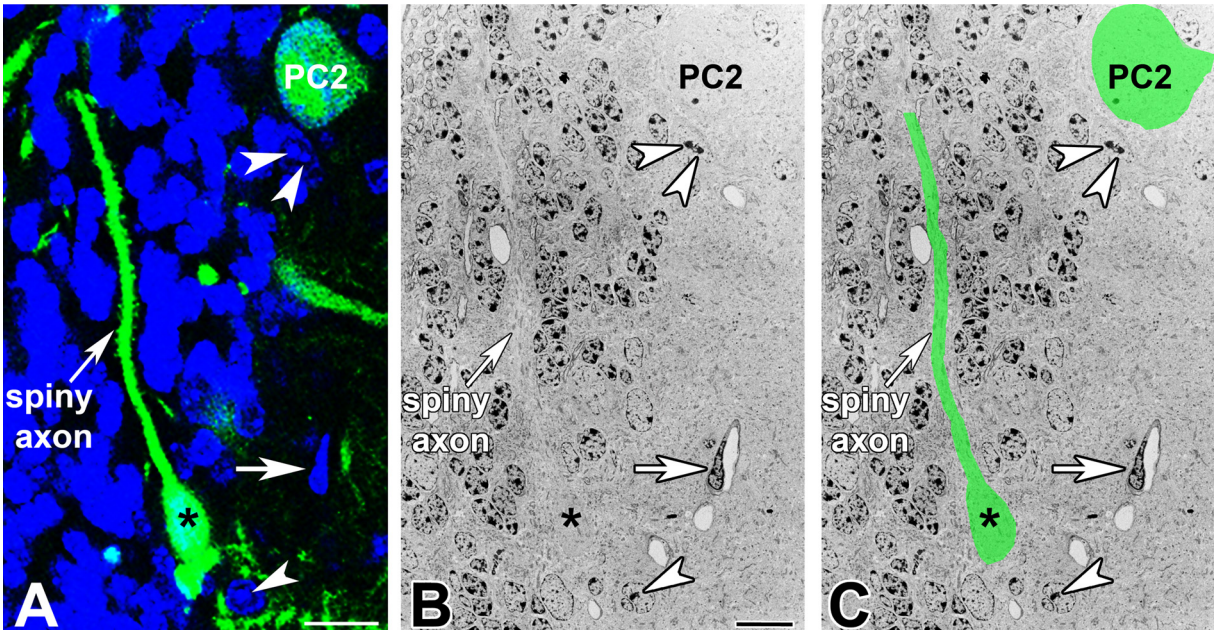

Fig. S4. Identification of an EGFP-positive spiny PC axon at the EM level. (*A*) Confocal image of EGFP-positive spiny axon and surrounding nuclei (labeled in blue by TO-PRO-3). A spiny axon can be traced from its corresponding PC soma (asterisk) into the deep granule cell layer. (*B*) At the EM level, the same spiny axon can be identified in ultrathin sections. Structures that can be matched between *A* and *B* include another PC soma (PC2), a nucleus of a vascular endothelial cell (arrow), and distinct nucleoli of Bergmann glia (arrowheads). The plane of the ultrathin section thus precisely corresponds to that recorded by confocal microscopy in *A*. (*C*) The contours of the correlated spiny axon and the second PC soma (PC2) are highlighted in green. The trajectory of the spiny axon exactly matches that shown in *A*. (Scale bars, 10 μm.)

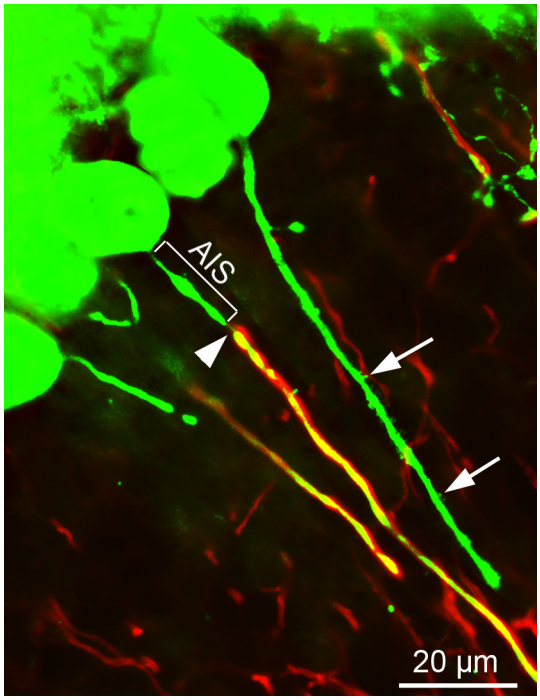

Fig. S5. Spiny axons of ankG$^{-/-}$ PCs exhibit impaired myelination as revealed by double immunofluorescence for calbindin (green) and myelin basic protein (red). Arrows point to a spiny axon that lacks a myelin sheath. By comparison, a neighboring nonspiny axon (arrowhead) is endowed with a normal myelin sheath.

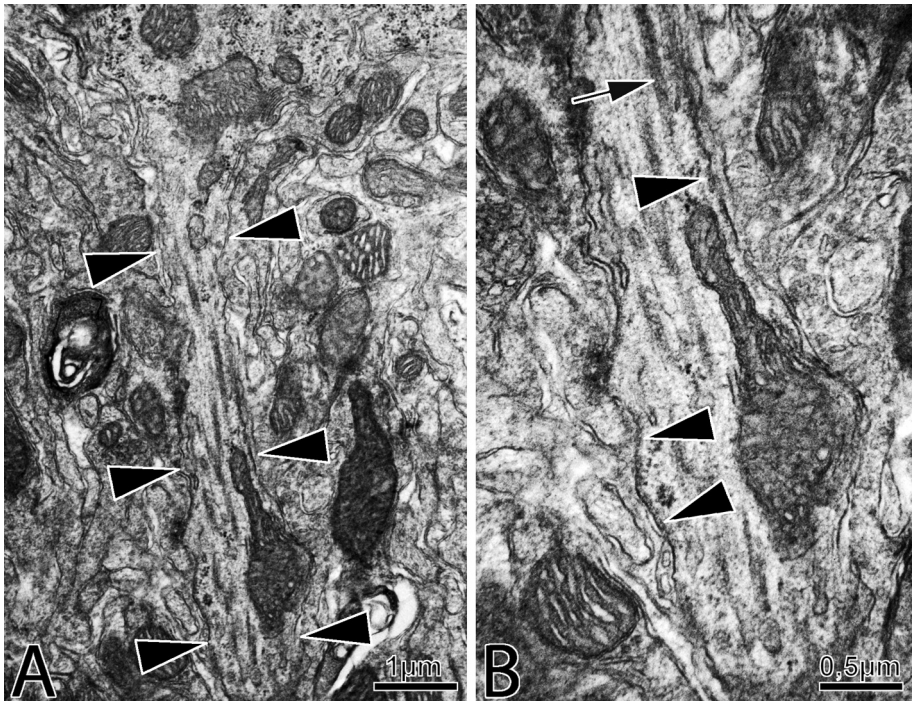

Fig. S6. Ultrastructural features of an AIS originating from a control PC. (*A*) The borders of the AIS are indicated by arrowheads. (*B*) Close-up view showing typical AIS features including the dense undercoating (arrowheads) and fasciculated microtubules (arrow).

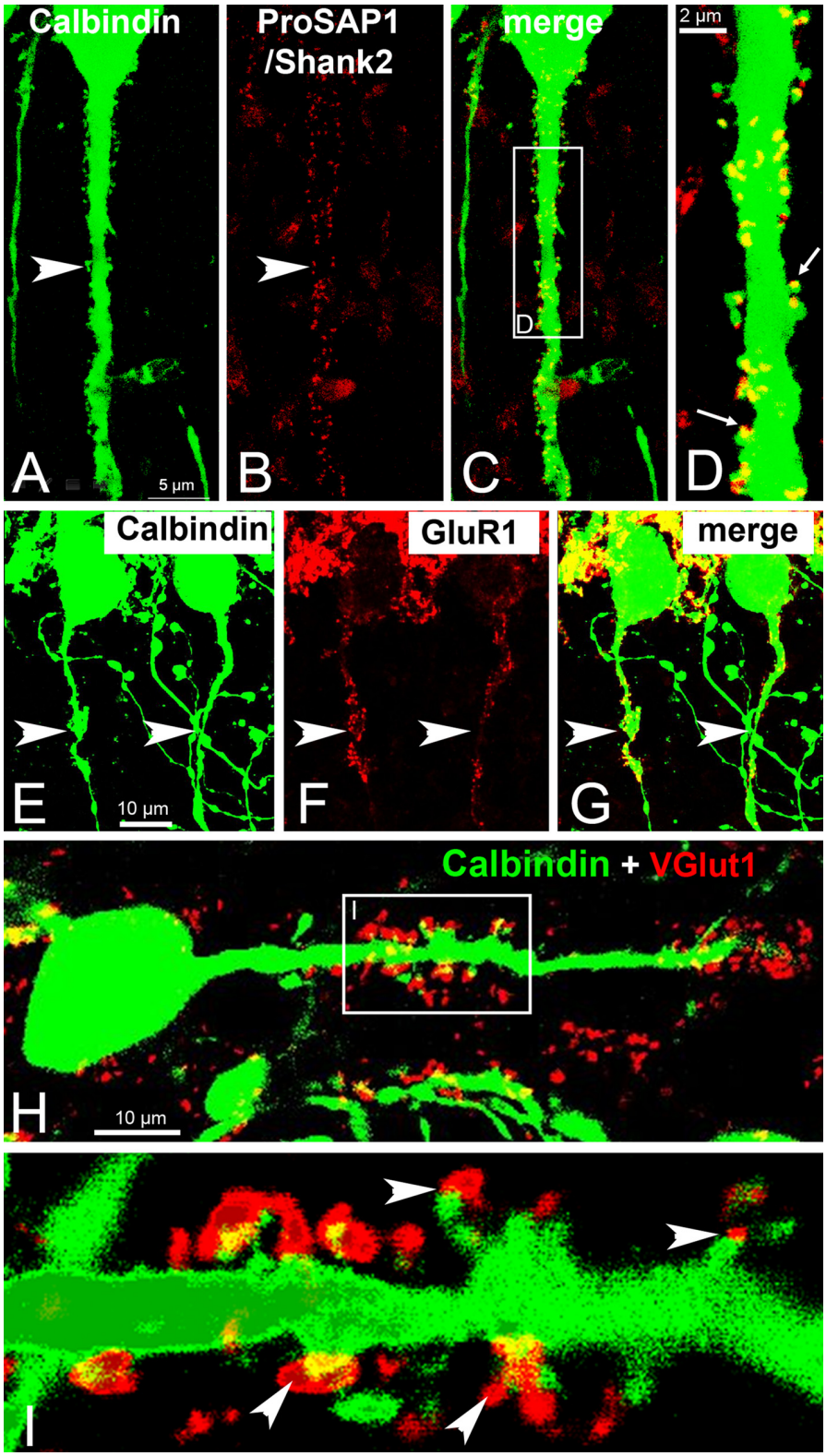

Fig. S7. EGFP-positive spiny PC axons in cerebellar slice cultures (DIV10) exhibit dendritic features. Cultures were prepared from L7-EGFP/ankG$^{-/-}$ mice at P9. (*A*–*D*) ProSAP1/Shank2 is targeted to an EGFP-positive spiny PC axon (arrowhead). (*D*) Close-up view of framed area in *C*. Arrows: accumulation of ProSap1/Shank2 in axonal spines. (*E*–G) EGFP-positive spiny axons are enriched with the ionotropic glutamate receptor GluR1 (arrowheads). (*H* and *I*) EGFP-positive axonal spines are contacted by VGlut1-positive boutons. A close-up view of the framed area in *H* is shown in *I*.